Tunable thermal links

C. W. Chang,[a] D. Okawa, H. Garcia, and T. D. Yuzvinsky
Department of Physics, University of California at Berkeley, California 94720 and Center of Integrated Nanomechanical Systems, University of California at Berkeley, California 94720

A. Majumdar
Department of Mechanical Engineering, and Department of Materials Science and Engineering, University of California at Berkeley, California 94720 and Materials Sciences Division, Lawrence Berkeley National Laboratory, Berkeley, California 94720

A. Zettl[b]
Department of Physics, University of California at Berkeley, California 94720 and Center of Integrated Nanomechanical Systems, University of California at Berkeley, California 94720 and Materials Sciences Division, Lawrence Berkeley National Laboratory, Berkeley, California 94720

(Received 28 February 2007; accepted 18 April 2007; published online 8 May 2007)

We demonstrate that the thermal conductance K of individual multiwall carbon nanotubes can be controllably and reversibly adjusted by sliding the outer shells of the tube with respect to the inner core in a telescopinglike manner. K shows an exponential dependence on the telescoping distance. Tunable nanoscale thermal links have immediate implications for nano- to macroscale thermal management, biosystems, and phononic information processing. © *2007 American Institute of Physics*. [DOI: 10.1063/1.2738187]

Unlike electrical conductivity which can vary by more than 27 orders of magnitude from insulators to metals, thermal conductivity varies by less than a factor of 10^4 at room temperature from the best thermal conductors to the best thermal insulators. In addition, unlike typical field-effect transistors for which the channel electrical conductance can change by more than a factor of 10^6, microelectromechanical-system-based contact/noncontact switches show only a 50% modulation of the thermal conductance.[1] This lack of variability and tunability of phonon transport in materials is a major obstacle for effective thermal management and processing of phonons as information carriers.

Multiwall carbon nanotubes (MWCNTs) comprise concentric cylindrical shells of strongly sp^2-bonded carbon atoms, where successive shells interact predominantly via weak van der Waals forces.[2] The large disparity between the strength of the in-plane sp^2 bonding and the van der Waals bonding has been exploited in the construction of various MWCNT-based nanoelectromechanical devices. For example, telescopically extended MWCNTs can serve as bearings,[3] rheostats,[4] and resonators,[5] with friction between shells measured to be less than $\sim 10^{-15}$ N/atom.[6]

MWCNTs with diameters ranging from 10 to 33 nm were prepared using conventional arc methods.[7] Individual tubes were placed on a custom designed microscale thermal conductivity test fixture using a piezodriven nanomanipulator operated inside an scanning electron microscope (SEM). Details of the test fixture fabrication process and measurement technique have been published elsewhere.[8] Two important extensions of the experimental method were employed for the present experiments. First, the test fixture incorporated a window directly below the MWCNT, facilitating direct high-resolution transmission electron microscope (TEM) imaging of the nanotube under study. Second, the two sample mounting pads of the fixture, between which the MWCNT was suspended, could be physically displaced relative to each other via an externally controlled nanomanipulator, allowing telescoping of the MWCNT during thermal conductivity measurements.

MWCNTs were bonded to the thermal source and sensor mounting pads of the test fixture using trimethyl cyclopentadienyl platinum ($C_9H_{16}Pt$) for mechanical strength and to reduce contact thermal resistance. The thermal conductance of individually suspended MWCNTs was determined from the known temperature gradient across the sample and the heat flow through the sample from the thermal source pad to the thermal sensor pad. The dimensions of the MWCNT were determined from SEM and associated high-resolution TEM images.

Figure 1 shows a SEM image of a MWCNT mounted between the test fixture thermal source and sensor pads. The nanotube is just visible in the center of the picture. The inset

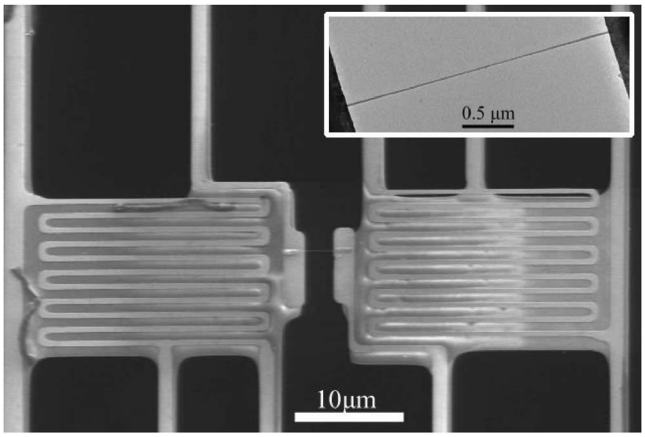

FIG. 1. SEM image of a MWCNT mounted between heater and sensor pads of the thermal test fixture (scale bar=10 μm). Inset: TEM image of the same MWCNT (scale bar=0.5 μm).

[a]Electronic mail: chihwei@berkeley.edu
[b]Electronic mail: azettl@berkeley.edu

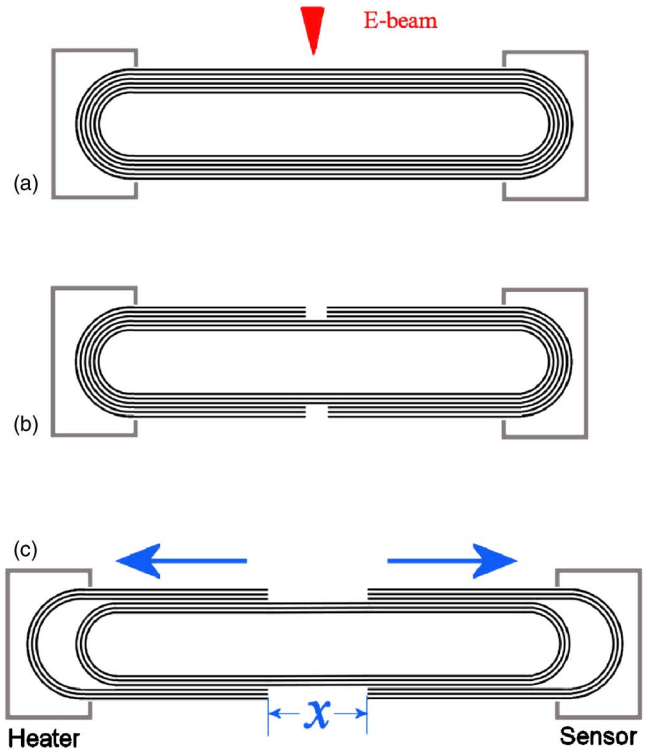

FIG. 2. (Color online) Schematic diagram of experimental procedures. [(a) and (b)] The outermost shells of a MWCNT are anchored to the electrodes, and then the middle section of the MWCNT is partially cut using the electron beam of a SEM. (c) A nanomanipulator (not shown) used to pull the suspended electrodes apart so that the released outer layers telescope away from each other. x is the telescoping distance.

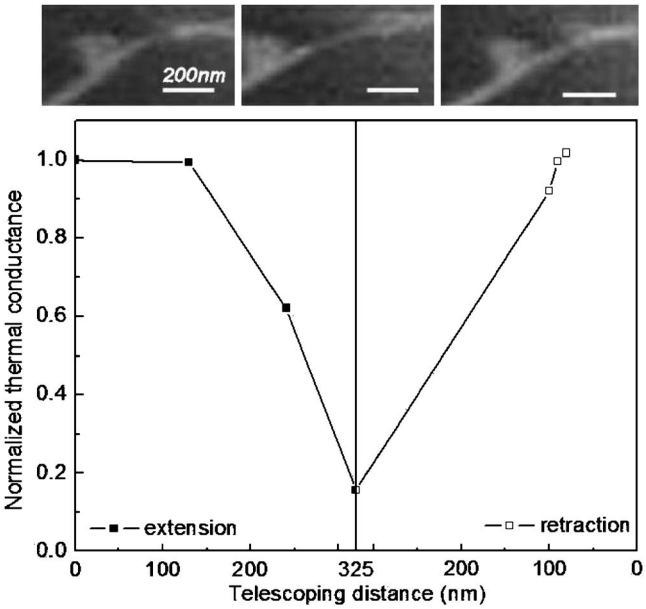

FIG. 3. Upper panel: SEM images of the MWCNT before extension (left), at the maximum extension (middle), and after retraction (right) (scale bar =200 nm). Lower panel: normalized thermal conductance vs distance x, for both telescopic extension (left panel) and telescopic retraction (right panel). The thermal conductance is normalized to the initial value of 4.4×10^{-9} W/K. The error bar (~3%) is less than the size of the symbol. For an extension of x=325 nm, the thermal conductance drops by 85%, but upon retraction it fully recovers to its former x=0 value. Note the mirror-image x-axis scale about the maximum extension at 325 nm.

to Fig. 1 shows a low-resolution TEM image of the same MWCNT. This particular nanotube has a length of 2.73 μm, seven walls, and inner and outer diameters of 7.2 and 9.6 nm, respectively.

To telescope the MWCNT, the entire sensor pad (right pad in Fig. 1, with meandering platinum thermal sensor and five flexible suspension arms attached) was displaced relative to the opposing thermal source pad using the nanomanipulator. Figure 2 shows schematically the telescoping procedure. To ensure consistent and controlled telescoping, the outer shells of the MWCNT were first structurally compromised by partially cutting through them with the SEM electron beam,[9] as indicated in Figs. 2(a) and 2(b). The cut was performed in high vacuum ($<5\times10^{-6}$ mbar) without any assist gases in order to maintain sample cleanliness. The MWCNT could then be cleanly fractured and smoothly telescoped by distance x, as shown in Fig. 2(c). The thermal conductance of the telescoped MWCNT was determined *in situ* for different fixed x (with x determined either indirectly from the nanomanipulator calibration or from direct SEM observations of the telescoping process). The constant retraction force provided by the van der Waals interaction between core and housing shells for the telescoped MWCNT ensured that thermal conductance measurements were not compromised by anomalous strain effects associated with changes in telescoping distance x.[3]

The upper part of Fig. 3 shows the SEM images of a MWCNT undergoing one cycle of telescopic extension and retraction. The x dependence of the thermal conductance for the telescoped MWCNT, normalized to K at x=0, is shown in the lower part of Fig. 3.[10] Data on the left half of the figure correspond to telescopic extension, while those on the right correspond to telescopic retraction. Figure 3 dramatically shows that K is very sensitive to telescopic extension; indeed, the datum at x=325 nm is only 15% of the $K(x=0)$ value. Equally important, the initial thermal conductance is fully recovered once the nanotube is retracted to its original length. Telescopic extension of MWCNTs is thus the basis for a highly tunable and reversible thermal link.

Previous TEM and electrical resistance experiments on telescoping nanotubes have demonstrated that the telescoping motion is virtually wear-free.[3,6] Hence, we expect that telescoped MWCNTs can be cycled many times with no degradation in thermal performance. In the present study, however, we observed the onset of hysteretic behavior in K after multiple cycles of the telescoping process. Subsequent TEM imaging confirmed that a layer of amorphous carbon material had deposited on the surface of the MWCNT due to hydrocarbon cracking in the SEM, preventing full retraction. Obviously such contamination would not occur under normal (*sans* e-beam) operation of a telescoping MWCNT thermal link.

We now turn to the functional form of $K(x)$ and the mechanism responsible for the thermal conductance changes with telescoping. A simplified classical thermal diffusion model based on geometry alone predicts that K should decrease by less than 23% after extending by 320 nm, much smaller than the observed decrease of 85%. Furthermore, finite element analyses based on thermal diffusive models consistently indicate that K should be linearly dependent on x, which qualitatively differs from our experimental result. The observed behavior of K is inconsistent with classical diffusion models.

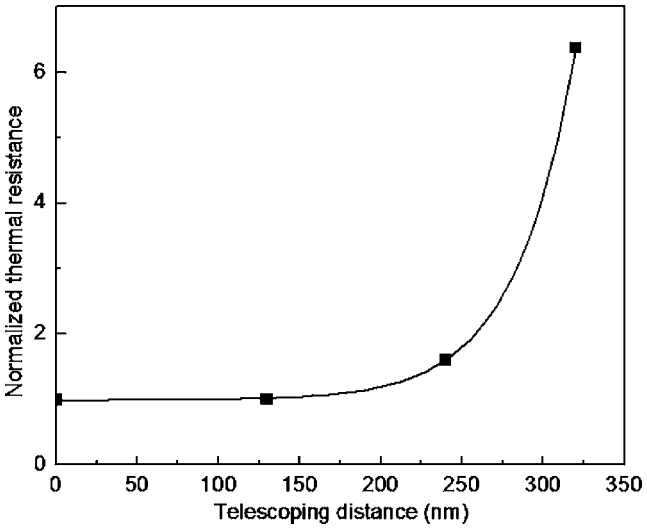

FIG. 4. Normalized thermal resistance R_T (inverse of K) vs telescoping distance x. The error bar ($\sim 3\%$) is less than the size of the symbol. The solid line is a fit to Eq. (1), with the characteristic electron localization length replaced by a phonon localization length $l_{ph}=74$ nm.

Figure 4 shows the normalized thermal resistance R_T $(=1/K)$ versus the telescoping distance x. Clearly R_T does not scale linearly with x nor can it be fitted by a parabolic curve. Previous electrical resistance measurements on telescopically extended MWCNTs have found an exponential form for the electrical resistance (R) behavior,

$$R(x) = R_0 \exp\left(\frac{2x}{l_e}\right), \tag{1}$$

where x is the telescoping distance and $l_e = 1000-1500$ nm is the electronic localization length.[4] The solid line in Fig. 4 is Eq. (1), with l_e replaced by a phononic localization length $l_{ph}=74$ nm, which is much shorter than l_e. This fit suggests that for MWCNTs, K is more sensitive to telescopic modulation than is the electrical resistance.

We now discuss several possible mechanisms that can lead to an exponentially sensitive K dependence on x. First, in analogy to localization of electrons,[4] the short l_{ph} is suggestive of phonons destructively interfering with each other during telescopic extension of the MWCNT, resulting in a dramatic reduction in K. This can happen when the phonon mean free path is larger than l_{ph}, and applies to our case where the pristine MWCNT has a phonon mean free path of ~ 200 nm.[10] Second, the tube-tube junction can form a tunable barrier that causes multiple phonon scatterings, leading to an exponential-like phonon transmission function in the Landauer-Buttiker formalism.[11] Theoretically, it has been shown that the thermal resistance between nanotubes is very sensitive to interfacial contacts.[12] Experimentally, it is found that the thermal conductivity of a MWCNT increases with reducing diameters, indicating intershell scattering to be the main phonon-phonon scattering mechanism.[13,14] These results would then suggest multiple phonon scatterings during telescoping. Third, the exponential dependence on x is reminiscent of the tunneling process ubiquitous in wave propagation. Because MWCNTs have a large anisotropy in the axial and the intershell coupling strength, phonon tunneling can result from the mismatches of these phonon modes. Thus, when a MWCNT is telescoped, the interfacial area becomes a variable-length barrier that effectively reduces the phonon transmission. This barrier can block the majority of phonons and can be as high as 50 meV, as indicated by the presence of phononic gaps in the phonon density of states of nanotubes.[15] Elucidating the dominating mechanism can further clarify the thermal transport phenomena in a MWCNT, but more experimental and theoretical works are needed.

From the application point of view, a controllable thermal switch, like a transistor in its electronic counterpart, will have great impact on thermal management in microelectronics, biosystems, and the field of phononics in general. Recently, solid state thermal rectifiers based on nanotubes have been demonstrated.[16] Theoretical proposals of thermal transistors and thermal rectifiers based on nonlinear control of the phononic band gap has been put forward.[17–19] A tunable thermal link, though now controlled by mechanical actuation, can actually be controlled by a thermal gate utilizing thermal expansion of materials. Our result is thus the first step toward a fully functional thermal transistor.

This work was supported in part by the Director, Office of Energy Research, Office of Basic Energy Sciences, Division of Materials Sciences, of the U.S. Department of Energy under Contract No. DE-AC03-7600098, and by the NSF within the Center of Integrated Nanomechanical Systems under Grant No. EEC-0425914.

[1] R. N. Supino and J. J. Talghader, Appl. Phys. Lett. **78**, 1778 (2001).
[2] S. Iijima, Nature (London) **354**, 56 (1991).
[3] J. Cumings and A. Zettl, Science **289**, 602 (2000).
[4] J. Cumings and A. Zettl, Phys. Rev. Lett. **93**, 086801 (2004).
[5] K. Jensen, C. Girit, W. Mickelson, and A. Zettl, Phys. Rev. Lett. **96**, 215503 (2006).
[6] A. Kis, K. Jensen, S. Aloni, W. Mickelson, and A. Zettl, Phys. Rev. Lett. **97**, 025501 (2006).
[7] D. T. Colbert, J. Zhang, S. M. McClure, P. Nikolaev, Z. Chen, J. H. Hafner, D. W. Owens, P. G. Kotula, C. B. Carter, J. H. Weaver, A. G. Rinzler, and R. E. Smalley, Science **266**, 1218 (1994).
[8] L. Shi, D. Y. Li, C. H. Yu, W. Y. Jang, D. Kim, Z. Yao, P. Kim, and A. Majumdar, J. Heat Transfer **125**, 881 (2003).
[9] T. D. Yuzvinsky, A. M. Fennimore, W. Mickelson, C. Esquivias, and A. Zettl, Appl. Phys. Lett. **86**, 053109 (2005).
[10] The thermal *conductivity* of the original MWCNT was measured to be 1100 W/m K at room temperature. After removing some of the outer shells by electron beam irradiation, the thermal conductivity was reduced to 380 W/m K, equivalent to $K=4.4\times10^{-9}$ W/K.
[11] P. G. Murphy and J. E. Moore, e-print, cond-mat/0701704.
[12] H. L. Zhong and J. R. Lukes, Phys. Rev. B **74**, 125403 (2006).
[13] C. W. Chang, A. M. Fennimore, A. Afanasiev, D. Okawa, T. Ikuno, H. Garcia, D. Y. Li, A. Majumdar, and A. Zettl, Phys. Rev. Lett. **97**, 085901 (2006).
[14] M. Fujii, X. Zhang, H. Q. Xie, H. Ago, K. Takahashi, T. Ikuta, H. Abe, and T. Shimizu, Phys. Rev. Lett. **95**, 065502 (2005).
[15] S. Rols, Z. Benes, E. Anglaret, J. L. Sauvajol, P. Papanek, J. E. Fischer, G. Coddens, H. Schober, and A. J. Dianoux, Phys. Rev. Lett. **85**, 5222 (2000).
[16] C. W. Chang, D. Okawa, A. Majumdar, and A. Zettl, Science **314**, 1121 (2006).
[17] B. W. Li, L. Wang, and G. Casati, Appl. Phys. Lett. **88**, 143501 (2006).
[18] B. W. Li, J. H. Lan, and L. Wang, Phys. Rev. Lett. **95**, 104302 (2005).
[19] B. W. Li, L. Wang, and G. Casati, Phys. Rev. Lett. **93**, 184301 (2004).